

## Factors Affecting Metal–Metal Bonding in the Face-Shared $d^3d^3$ Bioctahedral Dimer Systems, $MM'Cl_9^{5-}$ ( $M, M' = V, Nb, Ta$ )

Simon Petrie and Robert Stranger\*

Department of Chemistry, The Faculties, The Australian National University,  
Canberra ACT 0200, Australia

Received December 6, 2001

Density functional theory (DFT) calculations have been used to investigate the  $d^3d^3$  bioctahedral complexes,  $MM'Cl_9^{5-}$ , of the vanadium triad. Broken-symmetry calculations upon these species indicate that the V-containing complexes have optimized metal–metal separations of 3.4–3.5 Å, corresponding to essentially localized magnetic electrons. The metal–metal separations in these weakly coupled dimers are elongated as a consequence of Coulombic repulsion, which profoundly influences (and destabilizes) the gas-phase structures for such dimers; nevertheless, the intermetallic interactions in the V-containing dimers involve significantly greater metal–metal bonding character than in the analogous Cr-containing dimers. These observations all show good agreement with existing experimental (solid state) results for the chloride-bridged, face-shared dimers  $V_2Cl_9^{5-}$  and  $V_2Cl_3(thf)_6^+$ . In contrast to the V-containing dimers, complexes featuring only Nb and Ta have much shorter intermetallic distances ( $\sim 2.4$  Å) consistent with d-electron delocalization and formal metal–metal triple bond formation; again, good agreement is found with available experimental data. Calculations on the complexes  $V_2(\mu-Cl)_3(dme)_6^+$ ,  $Nb_2(\mu-dms)_3Cl_6^{2-}$ , and  $Ta_2(\mu-dms)_3Cl_6^{2-}$ , which are closely related to compounds for which crystallographic structural data exist, have been pursued and provide an insight into the intermetallic interactions in the experimentally characterized complexes. Analysis of the contributions from d-orbital overlap ( $E_{ovlp}$ ) stabilization, as well as spin polarization (exchange) stabilization of localized d electrons ( $E_{spe}$ ), has also been attempted for the  $MM'Cl_9^{5-}$  dimers. While  $E_{ovlp}$  clearly dominates over  $E_{spe}$  as a stabilizing factor in those dimers containing only Nb and Ta metal atoms, detailed assessment of the competition between  $E_{ovlp}$  and  $E_{spe}$  for V-containing dimers is obstructed by the instability of triply bonded V-containing dimers against Coulombic explosion. On the basis of the periodic trends in  $E_{ovlp}$  versus  $E_{spe}$ , the V-triad dimers have a greater propensity for metal–metal bonding than do their Cr-triad or Mn-triad counterparts.

### Introduction

The face-shared bioctahedral nonahalide complexes typified by  $Cr_2Cl_9^{3-}$  provide a very useful and sensitive structural prototype for investigating the factors influencing metal–metal bonding. The differences in total energy between structures possessing formal triple M–M bonds and those lacking any significant bonding interactions between the metal atoms are generally comparatively slight, and hence the degree of metal–metal bonding depends very strongly on parameters such as the spatial extent of the valence d orbitals. For example, experimental studies on the series of compounds  $M_2Cl_9^{3-}$  ( $M = Cr,^{1-5} Mo,^{6,7} W^{8-10}$ ) reveal that the

M–M interatomic distance decreases markedly from the chromium-containing dimer ( $r[Cr-Cr] \sim 3.10$  Å) to the tungsten-containing dimer ( $r[W-W] \sim 2.45$  Å), with a range of intermediate values being exhibited for  $Mo_2Cl_9^{3-}$ . This trend can be rationalized as arising from the greater efficiency of d-orbital overlap for the larger metal ions, resulting in a formal  $W \equiv W$  triple bond versus an essentially nonbonding  $Cr \cdots Cr$  interaction. Density functional theory (DFT) calculations on these compounds,<sup>11–15</sup> using the broken-symmetry

\* Author to whom correspondence should be addressed. E-mail: rob.stranger@anu.edu.au.

(1) Leuenberger, B.; Guedel, H. U. *Inorg. Chem.* **1986**, *25*, 181.

(2) Barry, K. R.; Maxwell, K. J.; Siddiqui, K. A.; Stevens, K. W. H. *J. Phys. C* **1981**, *14*, 1281.

(3) Wessel, G. J.; Ijdo, D. J. W. *Acta Crystallogr.* **1957**, *10*, 466.

(4) Cotton, F. A. *Rev. Pure Appl. Chem.* **1967**, *17*, 25.

(5) Grey, I. E.; Smith, P. W. *Aust. J. Chem.* **1971**, *24*, 73.

(6) Saillant, R.; Jackson, R. B.; Streib, W.; Foltling, K.; Wentworth, R. A. D. *Inorg. Chem.* **1971**, *10*, 1453.

(7) Stranger, R.; Smith, P. W.; Grey, I. E. *Inorg. Chem.* **1989**, *28*, 1271.

(8) Watson, W. H., Jr.; Waser, J. *Acta Crystallogr.* **1958**, *11*, 689.

(9) Stranger, R.; Grey, I. E.; Madsen, I. C.; Smith, P. W. *J. Solid State Chem.* **1987**, *69*, 162.

(10) Dunbar, K. R.; Pence, L. E. *Acta Crystallogr.* **1991**, *C47*, 23.

(11) Lovell, T.; McGrady, J. E.; Stranger, R.; Macgregor, S. A. *Inorg. Chem.* **1996**, *35*, 3079.

methodology,<sup>16</sup> are able to satisfactorily reproduce this trend, and provide a useful approach for extending the study of such complexes to species whose laboratory isolation has not yet been reported. In this manner, the influence of parameters such as charge state, halogen atom identity, d orbital occupancy, and transition metal atom row and group number on the tendency for metal–metal bond formation has been the subject of an ongoing computational study into such face-shared dimers.<sup>11–15,17–20</sup> While our earlier studies have encompassed d<sup>3</sup>d<sup>3</sup> face-shared dimers of the Cr and Mn triads,<sup>11–14</sup> and V/Cr and Cr/Mn mixed triad combinations,<sup>19,20</sup> as well as face-shared d<sup>1</sup>d<sup>1</sup> titanium triad and d<sup>2</sup>d<sup>2</sup> vanadium triad dimers,<sup>17</sup> we have not previously conducted any investigation of d<sup>3</sup>d<sup>3</sup> vanadium-triad dimers. Such a study is pertinent, however, since there are many examples known of face-shared d<sup>3</sup>d<sup>3</sup> dimers,<sup>21</sup> including vanadium-,<sup>22–26</sup> niobium-,<sup>27,28</sup> and tantalum-containing<sup>27</sup> species, while the magnetostructural properties of the V<sub>2</sub>Cl<sub>9</sub><sup>5-</sup> moiety (which has not itself been isolated) have been determined from analysis of V-doped metal halide crystals.<sup>1,29</sup> The available magnetic data<sup>1,29</sup> suggest that the magnetic coupling between V atoms in V<sub>2</sub>Cl<sub>9</sub><sup>5-</sup> is significantly greater than that evident in the isoelectronic Cr<sub>2</sub>Cl<sub>9</sub><sup>3-</sup> dimer. This trend is evident also in the magnetostructural survey of Wieghardt and co-workers,<sup>30</sup> who report that the experimental coupling constant for the crystallographically isolated (μ-Cl)<sub>3</sub> complex [(thf)<sub>3</sub>-VCl<sub>3</sub>V(thf)<sub>3</sub>]<sup>+</sup><sup>23</sup> is at least twice as large as that seen for several well-characterized halide-bridged face-sharing Cr<sub>2</sub> complexes. Nonetheless, the [(thf)<sub>3</sub>VCl<sub>3</sub>V(thf)<sub>3</sub>]<sup>+</sup> complex, currently one of only two d<sup>3</sup>d<sup>3</sup> face-shared V<sub>2</sub> complexes<sup>22,26</sup> to have been characterized by X-ray crystallography, is found to have too large a V–V separation (2.97–2.99 Å)<sup>22–25</sup> to indicate any significant degree of metal–metal bonding, in contrast to the existing (triply bonded) dinobium and ditantalum d<sup>3</sup>d<sup>3</sup> face-shared complexes.<sup>27,28</sup> The magnetic coupling in [(thf)<sub>3</sub>VCl<sub>3</sub>V(thf)<sub>3</sub>]<sup>+</sup> has been investigated by a theoretical study<sup>31</sup> on the model complex [(H<sub>2</sub>O)<sub>3</sub>VCl<sub>3</sub>V-

(OH)<sub>3</sub>]<sup>+</sup>. Finally, the metal–metal separation in [(thf)<sub>3</sub>V-(μ-Cl)(μ-CF<sub>3</sub>CO<sub>2</sub>)<sub>2</sub>V(thf)<sub>3</sub>]<sup>+</sup> has been found<sup>26</sup> to be much greater (3.796 Å), and the magnetic coupling constant substantially smaller, than the corresponding values for the analogous (μ-Cl)<sub>3</sub> complex.<sup>23</sup>

Many aspects of the trends in magnetic coupling seen in such dinuclear complexes can be very usefully probed by using density functional theory (DFT). Our previous studies on d<sup>3</sup>d<sup>3</sup> dimers of the Cr and Mn triads<sup>11–13,19</sup> have revealed a consistent correlation between the adjacent metal atoms' overlap energy  $E_{\text{ovlp}}$  and the spin polarization energy  $E_{\text{spe}}$ , where these parameters are defined respectively as the stabilization energies of the metal–metal triple bonded ( $S = 0$ ) and nonbonded ( $S = 3$ ) minima relative to the minimum found for a hypothetical “reference state” in which neither metal–metal bonding nor spin polarization of either metal atom's d electrons is permitted. Given the very strong correlation between  $E_{\text{ovlp}}$  and  $E_{\text{spe}}$  for the Cr and Mn triads, it was of considerable interest to us to determine whether this correlation was exhibited also by d<sup>3</sup>d<sup>3</sup> dimers of the vanadium triad. The present study examines this issue, and the general structural trends evident in these dimers, with use of the broken-symmetry (BS) methodology discussed in more detail below.

### Computational Details

All calculations described in this work were performed on Linux-based Pentium III 600 MHz computers with the Amsterdam Density Functional (ADF) program, version ADF2000,<sup>32</sup> developed by Baerends et al.<sup>33</sup> All calculations employed the local density approximation (LDA) to the exchange potential,<sup>34</sup> and the correlation potential of Vosko, Wilk, and Nusair.<sup>35</sup> Previous studies<sup>13,36–43</sup> and our own ongoing investigations<sup>44</sup> have shown that, for several classes of inorganic compounds but particularly for structural features of anionic metal-containing complexes,<sup>13,42,43</sup> the VWN implementation of the LDA generally offers significantly better agreement with experimental geometries (in relation to metal–metal

- (12) McGrady, J. E.; Lovell, T.; Stranger, R. *Inorg. Chem.* **1997**, *36*, 3242.  
 (13) McGrady, J. E.; Stranger, R.; Lovell, T. *J. Phys. Chem. A* **1997**, *101*, 6265.  
 (14) McGrady, J. E.; Stranger, R.; Lovell, T. *Inorg. Chem.* **1998**, *37*, 3802.  
 (15) Stranger, R.; Turner, A.; Delfs, C. D. *Inorg. Chem.* **2001**, *40*, 4093.  
 (16) Noodleman, L. *J. Chem. Phys.* **1981**, *74*, 5737.  
 (17) Stranger, R.; McGrady, J. E.; Lovell, T. *Inorg. Chem.* **1998**, *37*, 6795.  
 (18) Lovell, T.; Stranger, R.; McGrady, J. E. *Inorg. Chem.* **2001**, *40*, 39.  
 (19) Petrie, S.; Stranger, R. *Polyhedron* **2002**, *21*, 1163.  
 (20) Petrie, S.; Stranger, R. *Inorg. Chem.* **2002**, *41*, 2341.  
 (21) Cotton, F. A.; Walton, R. A. *Multiple Bonds between Metal Atoms*, 2nd ed.; Clarendon Press: Oxford, 1993.  
 (22) Cotton, F. A.; Duraj, S. A.; Extine, M. W.; Lewis, G. E.; Roth, W. J.; Schmulbach, C. D.; Schwotzer, W. *J. Chem. Soc., Chem. Commun.* **1983**, 1377.  
 (23) Bouma, R. J.; Teuben, J. H.; Beukema, W. R.; Bansemmer, R. L.; Huffman, J. C.; Caulton, K. G. *Inorg. Chem.* **1984**, *23*, 2715.  
 (24) Cotton, F. A.; Duraj, S. A.; Roth, W. J. *Inorg. Chem.* **1985**, *24*, 913.  
 (25) Canich, J. A. M.; Cotton, F. A.; Duraj, S. A.; Roth, W. J. *Polyhedron* **1987**, *6*, 1433.  
 (26) Gelmini, L.; Armstrong, W. H. *J. Chem. Soc., Chem. Commun.* **1989**, 24, 1904.  
 (27) Cotton, F. A.; Diebold, M. P.; Roth, W. J. *J. Am. Chem. Soc.* **1987**, *109*, 5506.  
 (28) Cotton, F. A.; Shang, M. *Inorg. Chim. Acta* **1994**, 227, 191.  
 (29) Riesen, H.; Guedel, H. U. *Inorg. Chem.* **1984**, *23*, 1880.  
 (30) Niemann, A.; Bossek, U.; Wieghardt, K.; Butzlaff, C.; Trautwein, A. X.; Nuber, B. *Angew. Chem., Int. Ed. Engl.* **1992**, *31*, 311.

- (31) Ratikin, Y. V.; Vetrov, A. V.; Kalinnikov, V. T. *Zh. Neorg. Khim.* **1996**, *41*, 642.  
 (32) Baerends, E. J.; Bérces, A.; Bo, C.; Boerrigter, P. M.; Cavallo, L.; Deng, L.; Dickson, R. M.; Ellis, D. E.; Fan, L.; Fischer, T. H.; Fonseca Guerra, C.; van Gisbergen, S. J. A.; Groeneveld, J. A.; Gritsenko, O. V.; Harris, F. E.; van den Hoek, P.; Jacobsen, H.; van Kessel, G.; Kootstra, F.; van Lenthe, E.; Osinga, V. P.; Philipsen, P. H. T.; Post, D.; Pye, C.; Ravenek, W.; Ros, P.; Schipper, P. R. T.; Schreckenbach, G.; Snijders, J. G.; Sola, M.; Swerhone, D.; te Velde, G.; Vernooijs, P.; Versluis, L.; Visser, O.; van Wezenbeeck, E.; Wiesenekker, G.; Wolff, S. K.; Woo, T. K.; Ziegler, T.; ADF2000.01.  
 (33) Fonseca Guerra, C.; Snijders, J. G.; te Velde, G.; Baerends, E. J. *Theor. Chem. Acc.* **1998**, *99*, 391.  
 (34) Parr, R. G.; Yang, W. *Density Functional Theory of Atoms and Molecules*; Oxford University Press: New York, 1989.  
 (35) Vosko, S. H.; Wilk, L.; Nusair, M. *Can. J. Chem.* **1980**, *58*, 1200.  
 (36) Daul, C.; Baerends, E. J.; Vernooijs, P. *Inorg. Chem.* **1994**, *33*, 3538.  
 (37) Rogemond, F.; Chermette, H.; Salahub, D. R. *Chem. Phys. Lett.* **1994**, *219*, 228.  
 (38) Deeth, R. J.; Jenkins, H. D. B. *J. Phys. Chem. A* **1997**, *101*, 4793.  
 (39) Doclo, K.; de Corte, D.; Daul, C.; Güdel, H. U. *Inorg. Chem.* **1998**, *37*, 3842.  
 (40) Besançon, K.; Laurency, G.; Lumini, T.; Roulet, R.; Bruyndonckx, R. *Inorg. Chem.* **1998**, *37*, 5634.  
 (41) Bendix, J.; Deeth, R. J.; Weyhermüller, T.; Bill, E.; Wieghardt, K. *Inorg. Chem.* **2000**, *39*, 930.  
 (42) Bridgeman, A. J.; Cavigliasso, G. *J. Phys. Chem. A* **2001**, *105*, 7111.  
 (43) Bridgeman, A. J.; Cavigliasso, G. *Polyhedron* **2001**, *20*, 2269.  
 (44) Petrie, S.; Stranger, R. *J. Phys. Chem. A*, submitted for publication.

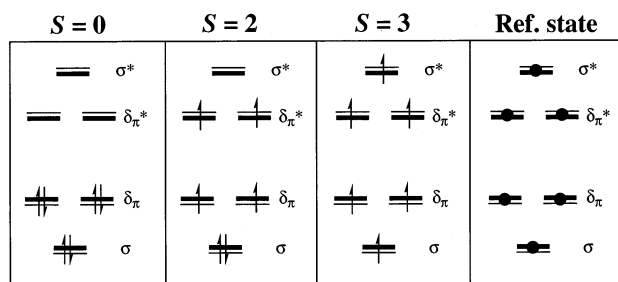


**Figure 1.** Representation of  $t_{2g}$ -derived orbital occupancy for the  $S = 0$ , 2, and 3 associated states, and for the reference state, for a face-shared  $d^3d^3$  dimer  $M_2Cl_9^{5-}$ .

distances) than do more computationally demanding DFT calculations incorporating nonlocal corrections to the exchange potential. Basis sets for all atoms were of triple- $\zeta$  quality with Slater-type orbitals. Electrons in orbitals up to and including 2p {Cl, V}, 3d {Nb}, and 4d {Ta} were treated in accordance with the frozen-core approximation. Optimized geometries were obtained with use of the gradient algorithm of Versluis and Ziegler.<sup>45</sup> Full-symmetry calculations for the  $S = 0$ , 2, and 3 associated states, “reference state” calculations of the type described previously,<sup>12</sup> and broken-symmetry (BS) calculations for the  $M_S = 0$  state (employing an asymmetry in the initial spin densities upon the two metal atoms)<sup>46</sup> were performed in a spin-unrestricted manner with  $D_{3h}$  or  $C_{3v}$  symmetry for the associated states and reference state ( $C_{3v}$  was always employed for the BS calculations). Potential energy curves for all pertinent states were obtained by optimization of all other structural parameters for the dimers along a series of fixed metal–metal separations.

## Results and Discussion

**Intermetallic Bonding versus Weak Coupling: A Brief Overview.** The various feasible metal–metal interactions in a  $d^3d^3$  face-shared dimer, viz., triple M–M bond formation, single M–M bonding, and weak magnetic coupling between the two metal atoms, can satisfactorily be modeled in calculations in which the valence d-orbital occupations are constrained to yield the appropriate M–M bond order upon optimization. The six valence electrons—two in  $a_1$ -symmetry and four in  $e$ -symmetry orbitals, where these orbitals are the reduced-symmetry analogues of the  $t_{2g}$  manifold of an octahedral complex—can participate in  $\sigma$  ( $a_1$ ) and  $\delta_{\pi}$  ( $e$ ) bonding if electron pairing is permitted, as is the case in a calculation on the  $S = 0$  associated state (see Figure 1). Also shown in this figure are the occupations assigned for the  $S = 2$  associated state, in which  $\sigma$  but not  $\delta_{\pi}$  bonding is permitted, yielding a single M–M bond; the  $S = 3$  associated state, wherein alignment of all electrons enforces a weakly coupled (ferromagnetic) dimer; and the so-called “reference state”, in which each occupied orbital contains half an  $\alpha$ -spin, and half a  $\beta$ -spin, electron. As discussed previously,<sup>12</sup> the purpose of the “reference state” in our calculations is to model a hypothetical dimer for which neither stabilization by metal–metal bonding nor stabilization by spin-polarization splitting of the  $\alpha$ - and  $\beta$ -spin-orbitals on either metal center is permitted. These concepts have been explored in greater detail in several of our previous studies on face-shared dimers.<sup>12,13</sup>

(45) Versluis, L.; Ziegler, T. J. *J. Chem. Phys.* **1988**, *88*, 322.

(46) Noodleman, L.; Norman, J. G., Jr. *J. Chem. Phys.* **1979**, *70*, 4903.

**Methodological Considerations: Core Sizes, Imposed Symmetry, and Complex Stability against Fragmentation.** Our initial calculations using standard frozen cores, for example, [1s 2s 2p 3s 3p] for vanadium, led to anomalous behavior (exhibited only at short intermetallic separations) for the V-containing complexes. This appeared to arise from an inversion of the vanadium 3p (“core”) and chlorine 3s (“valence”) orbital energies at close V–M distances, leading to inappropriate orbital assignment in the frozen-core DFT calculations on V-containing complexes. (In practice, this manifested itself solely during the optimizations on the  $S = 0$  associated state for the various  $VM'Cl_9^{5-}$  species). Similar problems with “routine” assignment of the frozen core, in ab initio calculations involving both metallic and highly electronegative atoms, have been encountered previously by a number of authors,<sup>47–53</sup> and this problem can usually be redressed by excluding from the frozen core those atomic orbitals nearest in energy to any of the valence orbitals. In the present study, this was done by adopting cores of [1s 2s 2p] for V and Cl, [1s 2s 2p 3s 3p 3d] for Nb, and [1s 2s 2p 3s 3p 3d 4s 4p 4d] for Ta.

The core-size modifications described above satisfactorily rectified the core/valence orbital energy problems. However, a further problem arising in some calculations was the instability of the isolated  $MM'Cl_9^{5-}$  pentaanion against concerted loss of several  $Cl^-$  ions. All calculations were performed in  $C_{3v}$  or  $D_{3h}$  symmetry, ensuring that the only available means for reducing Coulombic repulsion was the simultaneous expulsion of a symmetry-related set of terminal  $Cl^-$  ions. Calculations in which this occurred (invariably only for comparatively short metal–metal separations, i.e.,  $r_{M-M} < 2.4$  Å) were the  $S = 0$  associated states of  $V_2Cl_9^{5-}$ ,  $VNbCl_9^{5-}$ ,  $VTaCl_9^{5-}$ , and  $NbTaCl_9^{5-}$  and the BS ( $M_S = 0$ ) state of  $NbTaCl_9^{5-}$ . While  $S = 0$   $V_2Cl_9^{5-}$  lacked a barrier to the symmetric detachment of all six terminal  $Cl^-$  ions, the problematic heterodinuclear complexes were not bound against  $3Cl^-$  loss from the lighter metal atom. Furthermore, a reduction in symmetry in the  $Nb_2Cl_9^{5-}$  and  $Ta_2Cl_9^{5-}$   $S = 0$  complexes, from  $D_{3h}$  to  $C_{3v}$ , was found to significantly destabilize these complexes against Coulombic explosion: in  $D_{3h}$  symmetry these species possessed well-behaved minima, but in  $C_{3v}$  symmetry the niobium dimer lacked any barrier to symmetric loss of three terminal  $Cl^-$  ions from one niobium, while the corresponding barrier height for the tantalum dimer was only  $\sim 1.3$  kJ mol<sup>-1</sup>.

An obvious consequence of the Coulombic instability of these pentaanions in  $C_{3v}$  symmetry was to preclude characterization of optimized minima for some spin states. We have nevertheless attempted to obtain energetic data for these unstable configurations. For example, for  $V_2Cl_9^{5-}$  an ideal-

(47) Hofmann, H.; Hänsele, E.; Clark, T. J. *Comput. Chem.* **1990**, *11*, 1147.

(48) Blaudeau, J.-P.; McGrath, M. P.; Curtiss, L. A.; Radom, L. *J. Chem. Phys.* **1997**, *107*, 5016.

(49) Duke, B. J.; Radom, L. *J. Chem. Phys.* **1998**, *109*, 3352.

(50) Kozelka, J.; Berges, J. *J. Chim. Phys. Phys. Chim. Biol.* **1998**, *95*, 2226.

(51) Petrie, S. J. *Phys. Chem. A* **1998**, *102*, 6138.

(52) Bauschlicher, C. W., Jr.; Melius, C. F.; Allendorf, M. D. *J. Chem. Phys.* **1999**, *110*, 1879.

(53) Ma, N. L.; Siu, F. M.; Tsang, C. W. *Chem. Phys. Lett.* **2000**, *322*, 65.

**Table 1.** Energetic and Structural Parameters for  $S = 0, 2,$  or  $3$ , Reference State, and Broken Symmetry (BS) Minima for Each Dimer System

MM' <sup>a</sup>	$E_{\text{rel}}(S=0)^b$	$r_0(\text{M}-\text{M})^c$	$E_{\text{rel}}(S=2)^b$	$r_2(\text{M}-\text{M})^c$	$E_{\text{rel}}(S=3)^b$	$r_3(\text{M}-\text{M})^c$	$E_{\text{rel}}(\text{ref})^{b,d}$	$E_{\text{tot}}(\text{BS})^e$	$r_{\text{BS}}(\text{M}-\text{M})^c$
VV	1.393 <sup>f,g</sup>	2.106 <sup>f,g</sup>	0.809	2.904	0.010	3.519	3.534	-31.002	3.413
VNb	0.399 <sup>g,h</sup>	2.255 <sup>g,h</sup>	0.387	2.987	0.024	3.669	2.937	-31.835	3.464
VTa	0.212 <sup>g,h</sup>	2.277 <sup>g,h</sup>	0.308	2.987	0.023	3.685	2.818	-31.720	3.464
NbNb	0.000	2.386	0.630	3.033	0.750	3.804	3.068	-33.316	2.387
NbTa	0.021 <sup>g,i</sup>	2.391 <sup>g,h</sup>	0.767 <sup>i</sup>	3.032	0.982 <sup>i</sup>	3.814	3.220 <sup>j</sup>	-33.423 <sup>g,h</sup>	2.388
TaTa	0.000	2.413	0.851	3.030	1.163	3.824	3.280	-33.474	2.412

<sup>a</sup> Identity of the two metal atoms M and M' in the bioctahedral complex MM'Cl<sub>9</sub><sup>5-</sup>. <sup>b</sup> Relative energy of the indicated state,  $E_{\text{rel}} = E_{\text{tot}} - E_{\text{tot}}(\text{BS})$ , in electronvolts. <sup>c</sup> Optimized intermetallic separation for the  $S = 0, 2,$  or  $3$  state, in angstroms. <sup>d</sup> Intermetallic separations for the reference state are very similar to those found for the  $S = 3$  associated state. <sup>e</sup> Total bond energy,  $E_{\text{tot}}$ , of the broken-symmetry optimized geometry, in electronvolts. <sup>f</sup> The indicated species did not possess a local minimum in  $D_{3h}$  symmetry for this state. <sup>g</sup> Parameters in italics were estimated according to the method described in the text. <sup>h</sup> The indicated species did not possess a local minimum in  $C_{3v}$  symmetry for this state. <sup>i</sup> Determination of  $E_{\text{rel}}$  precluded by the instability of the broken-symmetry minimum against Coulombic explosion. See text for details.

ized triple V–V bonded geometry was obtained as follows: a linear transit calculation was performed, sampling a range of terminal V–Cl bond lengths from 2.65 to 3.1 Å in partially optimized V<sub>2</sub>Cl<sub>9</sub><sup>5-</sup> structures. A graph of total energy versus V–Cl distance for this calculation indicated a comparatively abrupt change at 2.88 Å from a steeply decreasing curve to a noticeably shallower and virtually linear distance/energy relationship, which we interpret as representing the bond distance at which bond compression per se ceases to destabilize the V/Cl interaction. Hence this comparatively large<sup>54</sup> V–Cl distance of 2.88 Å was selected as the effective terminal bond length to be used in a subsequent partial optimization of the  $S = 0$  associated state geometry. It is this latter calculation from which the total energy and M–M bond distance values, listed for  $S = 0$  V<sub>2</sub>Cl<sub>9</sub><sup>5-</sup> in Table 1, were obtained, and similar strategies were adopted for the other Coulombically unstable structures described in this table. Clearly such a method of characterization has its faults, but the parameters obtained by this method are nevertheless of some value in comparing bonding trends across the vanadium triad. Note that the estimated terminal V–Cl bond length of 2.88 Å, for  $S = 0$  V<sub>2</sub>Cl<sub>9</sub><sup>5-</sup>, fits well with the trend seen for calculated terminal M–Cl bond lengths for the “well-behaved” minima: 2.77 and 2.70 Å respectively for  $S = 2$  and  $S = 3$  V<sub>2</sub>Cl<sub>9</sub><sup>5-</sup>, 2.90, 2.82, and 2.78 Å for  $S = 0, 2,$  and  $3$  Nb<sub>2</sub>Cl<sub>9</sub><sup>5-</sup>, and 2.88, 2.81, and 2.76 Å for  $S = 0, 2,$  and  $3$  Ta<sub>2</sub>Cl<sub>9</sub><sup>5-</sup>. The lengthening of terminal Nb–Cl and Ta–Cl bonds with increasing metal–metal bond order arises, at least in part, as a result of increased Coulombic repulsion between negative charge centers in these pentaanions, and our estimated  $S = 0$  V–Cl bond length is entirely consistent with this phenomenon.

It remains apparent, nevertheless, that the influence of Coulombic repulsion in the optimized minima hampers comparison with the expected M<sub>2</sub>Cl<sub>9</sub><sup>5-</sup> structure in a crystalline environment, where surrounding counterions stabilize the pentaanionic M<sub>2</sub>Cl<sub>9</sub><sup>5-</sup> moiety against distortion and fragmentation. We have explored various approaches with the aim of calculating counterion-stabilized geometries for the M<sub>2</sub>Cl<sub>9</sub><sup>5-</sup> associated states and broken-symmetry states.

(54) This terminal V–Cl distance is notably elongated compared to the values of 2.47–2.48 Å which have been obtained crystallographically for bridging V–Cl separations in the experimentally studied d<sup>3</sup>d<sup>3</sup> vanadium face-shared dimers [(thf)<sub>3</sub>VCl<sub>3</sub>V(thf)<sub>3</sub>]<sup>2+</sup> and [(thf)<sub>3</sub>V(μ-Cl)(μ-CF<sub>3</sub>CO<sub>2</sub>)<sub>2</sub>V(thf)<sub>3</sub>]<sup>+</sup>.<sup>26</sup> Our bridging V–Cl for V<sub>2</sub>Cl<sub>9</sub><sup>5-</sup> is, at 2.374 Å, in satisfactory agreement with the experimental comparison values.

However, several obstacles to this aim have arisen. The most seemingly appropriate method of including countercharges, which is to surround M<sub>2</sub>Cl<sub>9</sub><sup>5-</sup> with partial charges at each crystallographically determined position for such countercharges, does not permit geometry optimization of the M<sub>2</sub>Cl<sub>9</sub><sup>5-</sup> structure; thus determination of the “corrected” geometry for each associated state becomes highly laborious and impractical. To obviate this problem, we have performed partial geometry optimizations, in which the M<sub>2</sub>Cl<sub>9</sub><sup>5-</sup> structure is allowed to relax within a rigid framework of K<sup>+</sup> counterions, but have found the resulting M<sub>2</sub>Cl<sub>9</sub><sup>5-</sup> geometries, and relative energies for the associated states, to be unacceptably sensitive to small shifts in the counterion framework. A further apparent strategy, that of optimizing the positions of the counterions as well as of the M<sub>2</sub>Cl<sub>9</sub><sup>5-</sup> structure, has not been explored because such a gas-phase K<sub>5</sub>M<sub>2</sub>Cl<sub>9</sub> “molecule” is a rather poor model for the long-range order of the bulk crystalline [K<sub>5</sub>M<sub>2</sub>Cl<sub>9</sub>] environment. We conclude that the broken-symmetry and associated state calculations on M<sub>2</sub>Cl<sub>9</sub><sup>5-</sup> remain the most reliable extant predictors of metal–metal bonding properties in compounds featuring such a structural subunit.

**Structural and Energetic Trends Evident in the Broken-Symmetry Calculations on V-Triad Dimers.** Key structural and energetic data for the V-triad dimers are presented in Table 1, while the covalency-corrected spin densities<sup>55</sup> for the  $S = 2, S = 3$  and BS minima are given in Table 2. It is apparent from these results that the general tendencies for the BS minima, namely, large metal–metal separations and nonzero spin densities for the V-containing dimers and shorter intermetallic distances (with  $\mu_{\text{spin}} = 0$  on metal atoms) for the dimers containing only Nb and Ta, are consistent with previous findings for the Cr- and Mn-triad dimers.<sup>11–14</sup> That is, the relatively compact d-orbitals of first-row transition metals preclude effective metal–metal bond formation and lead instead to dimers stabilized by weak antiferromagnetic coupling of the metal atoms' valence d electrons. Conversely, the more diffuse nature of second- and third-

(55) The raw Mulliken spin densities were corrected by a factor of  $3/\rho_{\text{M(oct)}}$ , where  $\rho_{\text{M(oct)}}$  is the Mulliken spin density obtained for the central metal atom within the isolated high-spin d<sup>3</sup> octahedral complex MCl<sub>6</sub><sup>n-</sup>. The purpose of this correction factor is to allow for the effect of M–Cl bond covalency within the octahedral complex: covalency reduces the spin density from the value of 3 expected for a purely ionic complex featuring a d<sup>3</sup> metal atom. We assume for simplicity that the extent of M–Cl bond covalency within the d<sup>3</sup>d<sup>3</sup> face-shared dimer is similar to that found for the octahedral complex.

**Table 2.** Mulliken Spin Densities Determined for  $S = 2$ ,  $S = 3$  and Broken-Symmetry Minima of the Vanadium–Triad Dimers, Adjusted for Metal–Ligand Bond Covalency

MM'	$S = 2^a$		$S = 3^a$		BS <sup>a</sup>		MCl <sub>6</sub> <sup>5-</sup> <sup>b</sup>	
	$\rho_{\text{spin}}(\text{M})$	$\rho_{\text{spin}}(\text{M}')$	$\rho_{\text{spin}}(\text{M})$	$\rho_{\text{spin}}(\text{M}')$	$\rho_{\text{spin}}(\text{M})$	$\rho_{\text{spin}}(\text{M}')$	$\rho_{\text{spin}}(\text{M})$	$\rho_{\text{spin}}(\text{M}')$
VV	1.97	1.97	2.98	2.98	2.92	-2.92	3.15	3.15
VNb	2.22	1.71	3.06	2.87	2.86	-2.84	3.15	3.06
VTa	2.22	1.70	3.10	2.83	2.84	-2.82	3.15	3.04
NbNb	1.95	1.95	2.96	2.96	0	0	3.06	3.06
NbTa	1.97	1.93	2.98	2.94	0	0	3.06	3.04
TaTa	1.95	1.95	2.97	2.97	0	0	3.04	3.04

<sup>a</sup> Covalency-corrected values. The method of covalency correction is described within the text. <sup>b</sup> Spin densities for the octahedral complexes; these values are not covalency-corrected.

**Table 3.** Comparison of Experimental Literature Values for Metal–Metal Separations in  $d^3d^3$  Face-Shared V-, Nb-, and Ta-Containing Complexes, with DFT Values for Analogous “Model” Compounds.

model <sup>a,b</sup>	$S = 0$		$S = 2$		$S = 3$		BS		lit. value	
	$r_{\text{M-M}}^c$	$E_{\text{rel}}^d$	$r_{\text{M-M}}^c$	$E_{\text{rel}}^d$	$r_{\text{M-M}}^c$	$E_{\text{rel}}^d$	$r_{\text{M-M}}^c$	$\mu_{\text{spin}}^e$	$r_{\text{lit}}(\text{M-M})^f$	complex <sup>b,g</sup>
[(dme) <sub>3</sub> VCl <sub>3</sub> V(dme) <sub>3</sub> ] <sup>+</sup>	2.11	0.832	2.66	0.446	3.11	0.238	2.83	±2.80	2.976–2.993 <sup>h</sup>	[(thf) <sub>3</sub> VCl <sub>3</sub> V(thf) <sub>3</sub> ] <sup>+</sup>
[Cl <sub>3</sub> Nb( $\mu$ -dms) <sub>3</sub> NbCl <sub>3</sub> ] <sup>2-</sup>	2.64	0.003	3.13	2.673	3.65	3.466	2.66	0	2.626–2.632 <sup>i,j</sup>	[Cl <sub>3</sub> Nb( $\mu$ -tht) <sub>3</sub> NbCl <sub>3</sub> ] <sup>2-</sup>
[Cl <sub>3</sub> Ta( $\mu$ -dms) <sub>3</sub> TaCl <sub>3</sub> ] <sup>2-</sup>	2.66	0.006	3.16	2.945	3.67	3.919	2.68	0	2.61 <sup>g</sup>	[Cl <sub>3</sub> Ta( $\mu$ -tht) <sub>3</sub> TaCl <sub>3</sub> ] <sup>2-</sup>

<sup>a</sup> Model compound employed for computational purposes. <sup>b</sup> Abbreviations used: thf = tetrahydrofuran; tht = tetrahydrothiofuran; dme = dimethyl ether; dms = dimethyl sulfide. <sup>c</sup> Optimized metal–metal distance, in angstroms, on the indicated associated state or broken symmetry state surface. <sup>d</sup> Energy of the indicated associated state minimum, in eV, relative to that of the broken-symmetry minimum. <sup>e</sup> Unpaired (Mulliken) electron spin density on each metal atom, for the broken-symmetry minimum. <sup>f</sup> Range of experimentally determined metal–metal bond lengths, in angstroms, from the indicated crystallographic studies. <sup>g</sup> Experimentally isolated complex, structurally related to the indicated model compound. <sup>h</sup> Reference 23. <sup>i</sup> Reference 27. <sup>j</sup> Reference 28.

transition row valence d orbitals promotes multiple metal–metal bond formation rather than weak coupling. This picture is also consistent with the available experimental data on face-shared  $d^3d^3$  dimers of the vanadium triad, which indicate large metal–metal distances ( $r_{\text{V-V}} = 2.971 \text{ \AA}$  in [(thf)<sub>3</sub>-VCl<sub>3</sub>V(thf)<sub>3</sub>]<sup>+</sup>)<sup>23</sup> and small spin exchange coupling constants<sup>1,26,29</sup> for divanadium complexes, and short (triple) metal–metal bonds (2.60–2.63  $\text{\AA}$ )<sup>27,28</sup> in the known dinio-bium and ditantalum complexes. Our calculated bond lengths appear to exaggerate the difference between nonbonded (V<sub>2</sub>) and triply bonded (Nb<sub>2</sub>, Ta<sub>2</sub>) dimers, compared with experiment. Most notable, in this respect, is our calculation of a  $\mu$ -(Cl)<sub>3</sub> V–V distance of 3.41  $\text{\AA}$ , 0.44  $\text{\AA}$  greater than that found experimentally in [(thf)<sub>3</sub>VCl<sub>3</sub>V(thf)<sub>3</sub>]<sup>+</sup>.<sup>23</sup> We ascribe this discrepancy as arising largely from the perturbing influence of Coulombic repulsion between bridging and terminal chloride ions in our vacuum-phase, pentaanionic complex V<sub>2</sub>Cl<sub>9</sub><sup>5-</sup>, which will act to distort our calculated geometry significantly away from the expected structure within an electrically neutral, extended crystalline lattice.<sup>56</sup> (It should be noted that this bridging/terminal repulsion, and our calculation of a long  $\mu$ -(Cl)<sub>3</sub> V–V bond, is not merely an artifact of the computational technique, but represents the expected intramolecular interaction within V<sub>2</sub>Cl<sub>9</sub><sup>5-</sup> in the gas phase, should it prove possible to generate such a highly charged gas-phase species via a laboratory technique.) This

(56) This mode of Coulombic repulsion exists also, for example, in Cr<sub>2</sub>Cl<sub>9</sub><sup>3-</sup>, but in the latter cluster the electrostatic stresses are systematically much smaller: ionic factors, such as the greater attraction between Cr<sup>III</sup> and Cl<sup>-</sup> than between V<sup>II</sup> and Cl<sup>-</sup>, play a part, as does the increased covalency of the Cr/ligand interaction, which will act to reduce the degree of negative charge localization on Cl atoms in the Cr dimer. The difference in magnitude of the total Coulombic repulsion, in V-triad pentaanionic and Cr-triad trianionic dimers, can be appreciated via the observation that spontaneous loss of Cl<sup>-</sup> ions was not seen in any of our calculations on the Cr-triad dimers.<sup>11–13</sup>

bridging/terminal repulsion is essentially absent in the monocationic [(thf)<sub>3</sub>VCl<sub>3</sub>V(thf)<sub>3</sub>]<sup>+</sup> complex, and it is therefore likely that the experimental value,<sup>23</sup> which we are satisfactorily able to model (see Table 3 and the discussion below), is much more representative of solid-state V<sup>II</sup>–V<sup>II</sup> separations.

Comparison of the  $S = 2$ ,  $S = 3$  and BS covalency-corrected spin densities (see Table 2) yields some points of note. The metal atom spin densities for V<sub>2</sub>Cl<sub>9</sub><sup>5-</sup>, Nb<sub>2</sub>Cl<sub>9</sub><sup>5-</sup>, NbTaCl<sub>9</sub><sup>5-</sup>, and Ta<sub>2</sub>Cl<sub>9</sub><sup>5-</sup> all conform extremely closely to the expected values<sup>57</sup> assuming that d-electron content is shared equally between the two metals. There is, however, a tendency evident in the  $S = 2$  and 3 VNbCl<sub>9</sub><sup>5-</sup> and VTaCl<sub>9</sub><sup>5-</sup> dimers for a markedly greater d-electron content on V than on Nb or Ta, i.e., a modest degree of electron transfer from the heavier metal atom to V. Such a transfer is consistent with the larger spin polarization stabilization energy ( $E_{\text{sp}}$ ) for first-row than for second- or third-row transition metals (in a sense, the  $S = 2$  spin densities can be considered to represent a “weak push” toward a  $d^5d^1$  configuration featuring high-spin V<sup>0</sup>) and echoes also our previously reported findings of spin-density disparities between Cr<sup>III</sup> and W<sup>III</sup> in the  $S = 2$  and 3 associated state minima of the face-shared CrWCl<sub>9</sub><sup>3-</sup> complex.<sup>20</sup> Note also that the spin densities for BS minima of the V-containing complexes are uniformly slightly smaller in magnitude than the values for the corresponding  $S = 3$  minima, suggesting that some tendency toward weak metal–metal bonding is operating in these BS minima (such covalent bonding is effectively prevented in the  $S = 3$  associated state by alignment of all

(57) That is, spin densities of +2 and +3, respectively, on each metal in the  $S = 2$  ( $\sigma$ -bonded) and  $S = 3$  (nonbonded) structures, and an evenhanded distribution of the nonbonding electron density in the BS minimum, which can range from triply bonded (no nonbonding d electrons) to nonbonded (all six d electrons nonbonding).

the valence d-electrons). This interpretation is supported by examination of the BS and  $S = 3$  M–M distances for the V-containing dimers: for  $\text{VNbCl}_9^{5-}$  and  $\text{VTaCl}_9^{5-}$  in particular, the BS intermetallic separations are significantly smaller than the  $S = 3$  counterparts. The inference toward weakly bonding interactions between metal atoms in the V-containing complexes, while such interactions appear largely absent in analogous Cr-containing complexes according to our calculations,<sup>11–13</sup> compares favorably with the results of magnetochemical studies which have found substantially larger coupling constants for chloride-bridged, face-shared  $\text{V}_2$  complexes<sup>1,30</sup> than for analogous  $\text{Cr}_2$  complexes.

A direct comparison of experimental and computed geometries for the  $\text{M}_2\text{Cl}_9^{5-}$  complexes is prevented by the absence of crystallographic data on these species. However, as noted in the Introduction, there are several examples of V-, Nb-, and Ta-containing  $d^3d^3$  face-shared dimers of various formulas, and to further assess the reliability of our calculations we have performed BS and associated-state optimizations on the more highly symmetric examples of such compounds, as detailed in Table 3. The agreement between experiment and theory is good, and it is particularly pleasing to note that our V–V distance (of 2.83 Å) in the (monocationic) model compound is acceptably close to the value of 2.98 Å around which the experimental V–V values are clustered. This result further strengthens our assertion, above, that the calculated gas-phase V–V distance in  $\text{V}_2\text{Cl}_9^{5-}$  (3.41 Å) is elongated as a result of the large Coulombic repulsion terms implicit in such a highly negatively charged complex. Our calculations on the broken symmetry state of the  $\text{V}_2$  model compound also yield (uncorrected) Mulliken spin densities of +2.80 and –2.80 on the two metal atoms: the slight reduction from the expected values of  $\pm 3$  for a dimer featuring fully localized valence-d electrons is in agreement with the experimental results which suggest that the intermetallic interaction falls far short of formal  $\sigma$ -bond formation.<sup>23,30</sup> Finally for the  $\text{V}_2$  model compound, we have obtained a potential energy curve for the BS state as a function of V–V distance (Figure 2): this curve also clearly demonstrates that the BS minimum falls at a distance intermediate between a fully localized ( $S = 3$ ) structure and one featuring a V–V  $\sigma$  bond ( $S = 2$ ). Note that, while the optimized BS V–V distance (2.83 Å) is much closer to the  $S = 2$  distance (2.66 Å) than to the  $S = 3$  value (3.11 Å), the total energy of the  $S = 3$  minimum lies considerably closer than that of  $S = 2$  to the BS surface. This latter observation is consistent with the calculated spin densities which indicate only a relatively weak  $\sigma$  bonding interaction between the V atoms. The small energy separation between  $S = 2$  and  $S = 3$  minima (<0.2 eV) and the comparative shallowness of the observed broken symmetry minimum further suggest that the metal–metal interaction in this vanadium dimer cation may be rather sensitive to structural influences such as changing the counterions or modifying the terminal O-atom donor ligands (e.g. from water to methanol to dimethyl ether to tetrahydrofuran). This apparent sensitivity may merit a more detailed experimental investiga-

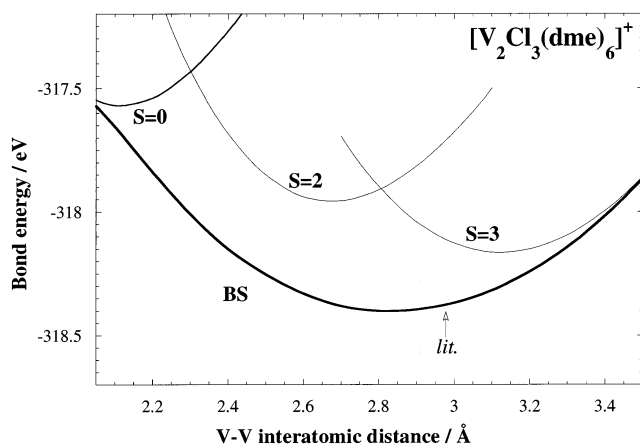


**Figure 2.** Potential energy curve, as a function of V–V internuclear separation, for the broken-symmetry state of the  $[(\text{dme})_3\text{V}(\mu\text{-Cl})_3\text{V}(\text{dme})_3]^+$  complex, with an arrow showing the experimentally obtained V–V bond distance for the analogous  $[(\text{thf})_3\text{V}(\mu\text{-Cl})_3\text{V}(\text{thf})_3]^+$  complex. Also shown are the curves due to the  $S = 0, 2$  and  $3$  associated states, in the vicinities of their respective minima.

tion of face-shared V(II) dimers, particularly since first-row face-sharing  $d^3d^3$  dimers featuring significant metal–metal bonding are notably scarce.<sup>21</sup>

In contrast to the results for the model vanadium dimer, the metal atom spin densities for the  $\text{Nb}_2$  and  $\text{Ta}_2$  models are found to be zero on each metal, supporting the assignment of a triple metal–metal bond in these systems.<sup>27,28</sup> These second- and third-row dimers also differ from the  $\text{V}_2$  model in that their various associated states ( $S = 0, 2$ , and  $3$ ) are widely spaced in an energetic sense: the  $S = 2$  and  $S = 3$  minima are simply too high in energy (relative to  $S = 0$ ) to have any significant influence on the BS minimum, which conforms almost completely to the  $S = 0$  structure. In this context also, the much better agreement between theoretical and experimental bond lengths for the  $\text{Nb}_2$  and  $\text{Ta}_2$  complexes (i.e., within 0.05 Å) than for  $\text{V}_2$  (where our theoretical result is  $\sim 0.15$  Å below crystallographic values for related compounds) is understandable given the apparent greater structural rigidity of the second- and third-row metal complex geometries.

**Localization versus Delocalization of the Metal-Based Electrons.** In previous studies on the Cr-triad, Mn-triad, and mixed-group  $d^3d^3$  face-shared dimers,<sup>11–15,17</sup> we have characterized the interplay between d-orbital overlap and spin polarization splitting as factors which respectively favor multiple metal–metal bonding or weak antiferromagnetic coupling in these dimers. Parametrization of these factors, as  $E_{\text{ovlp}} = E_{\text{ref}} - E_{S=0}$  and  $E_{\text{spe}} = E_{\text{ref}} - E_{S=3}$ , where  $E_{\text{ref}}$ ,  $E_{S=0}$ , and  $E_{S=3}$  are the energies of the respective minima for the reference state,  $S = 0$ , and  $S = 3$  associated state potential energy surfaces,<sup>12</sup> gives a quantitative measure of the stabilization due to metal–metal bond formation through d-orbital overlap, and of stabilization due to spin polarization of localized d-orbital electrons. Plots of  $E_{\text{ovlp}}$  versus  $E_{\text{spe}}$  for the same-group dimers of the  $\text{Cr}^{\text{III}}$  and  $\text{Mn}^{\text{IV}}$  triads have revealed a consistent linear trend:<sup>12</sup> a large  $E_{\text{ovlp}}$  value is associated with small  $E_{\text{spe}}$  for a given dimer, and as  $E_{\text{ovlp}}$  is reduced,  $E_{\text{spe}}$  increases. A similar tendency, though less consistently linear due to the added influence of intermetallic

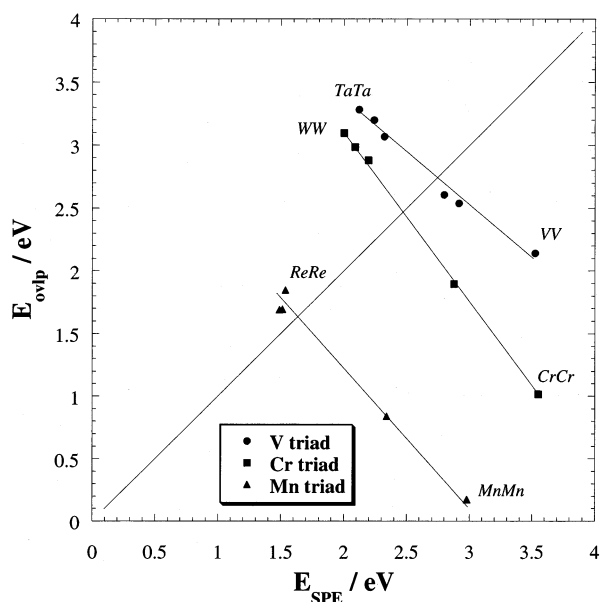


**Figure 3.** Graph of  $E_{\text{ovlp}}$  versus  $E_{\text{spe}}$  (see text for definitions) for the V, Cr, and Mn triad  $d^3d^3$  face-shared dimers. Best-fit lines show the general trend within each family; values for specific dimers are identified for the “terminal” members (i.e. homonuclear first-row and third-row dimers) of each triad. The diagonal bisecting the graph shows the boundary between  $S = 0$  and  $S = 3$  absolute stability, which reflects the tendency of dimers to form either multiple metal–metal bonds (upper left section) or weakly coupled complexes (lower right section).

electron transfer, is evident also for the mixed-group  $\text{V}^{\text{II}}/\text{Cr}^{\text{III}}$  and  $\text{Cr}^{\text{III}}/\text{Mn}^{\text{IV}}$  triad combinations.<sup>20</sup>

We have used the relative energies listed in Table 1 to obtain  $E_{\text{spe}}$  and  $E_{\text{ovlp}}$  values for the V-triad dimers, and these have been plotted in Figure 3, which includes also the Cr-triad and Mn-triad results. One important caveat regarding the V-triad data is that, for all of the V-containing complexes and for  $\text{NbTaCl}_9^{5-}$ , the  $E_{\text{ovlp}}$  values are not obtained from genuine minima on the appropriate  $S = 0$  associated state surface (because such minima do not exist according to our calculations) but are instead estimated from idealized geometries for these species. Nevertheless, the estimated  $E_{\text{ovlp}}$  values for the wayward V-triad complexes appear to fit very well the general trend exhibited by the other dimers on this graph: that is,  $E_{\text{ovlp}}$  increases at the expense of  $E_{\text{spe}}$  as one progresses from first-row toward third-row combinations within a given triad (with broadly comparable slopes seen for the best-fit lines for all three triads) and  $E_{\text{ovlp}}$  is systematically higher for V-triad dimers than for Cr-triad, and for Cr-triad than for Mn-triad dimers. A consequence of this trend in  $E_{\text{ovlp}}$  values across a transition row is that the heteronuclear V-containing nonachloride dimers are seen to lie much closer to the “boundary”, separating multiply bonded complexes from weakly coupled forms, than is the case for the analogous heteronuclear Cr- and Mn-containing complexes. Conversely, of all complexes in Figure 3 containing only second- or third-row transition metal atoms, it is the Mn-triad dimers which lie closest to this notional boundary. Thus we would expect that substitution of Cl bridges by another ligand might well have a better prospect for permitting weakly coupled  $\text{Re}_2$  dimers than for  $\text{W}_2$  or  $\text{Ta}_2$ , and this is precisely what is seen in calculations on the  $\text{M}_2\text{I}_9^{n-}$  ( $\text{M} = \text{W}^{\text{III}}, \text{Re}^{\text{IV}}$ ) dimers;<sup>15</sup> an analogous tendency is

apparent also for the  $\text{Mo}_2$  and  $\text{Tc}_2$  nonaiodides.<sup>15</sup> These trends can be rationalized as arising from two factors operating in concert: first, the d-orbital size decreases systematically as one progresses across a transition row, and second, the increasing charge on  $d^3$  metal atoms in going from left to right across a row induces yet greater d-orbital contraction. The ability of adjacent metal atoms to form effective metal–metal bonds is clearly dependent on the orbital size, with more diffuse orbitals promoting better overlap. A further extrapolation of these concepts, and their embodiment in Figure 3, is that it should be easier to induce  $\text{V}^{\text{II}}-\text{V}^{\text{II}}$  bonding, by ligand substitution, than  $\text{Cr}^{\text{III}}-\text{Cr}^{\text{III}}$  bonding, and we are currently investigating this notion. While the qualitative interrelationship between d-orbital size,  $E_{\text{ovlp}}$ , and  $E_{\text{spe}}$  is easily understood, a clear quantitative comprehension of this relationship remains elusive.

### Concluding Remarks

Bonding patterns seen in the  $d^3d^3$  face-shared dimers of the vanadium triad,  $\text{M}_2\text{Cl}_9^{5-}$ , largely match those which have been previously reported (and, in several instances, experimentally documented) for members of the Cr and Mn triads. The tendency toward weakly coupled dimers when at least one metal atom is first-row, and toward triple metal–metal bonding when only second- or third-row M is present, is also exhibited in the near-linear relationship between the overlap and spin polarization stabilization parameters  $E_{\text{ovlp}}$  and  $E_{\text{spe}}$ , in a manner consistent also with our previous calculations on the Cr and Mn triad dimers. Our calculations show evidence of a significantly greater degree of magnetic coupling in V-containing dimers than in analogous Cr-containing dimers, and this too is consistent with observed experimental trends. However, it appears also that Coulombic repulsion between negative charge centers is a major “perturbing influence” in our calculations on these pentaanionic complexes. This is most obviously manifested by the instability of several of the triply bonded dimers against multiple  $\text{Cl}^-$  loss, but is perhaps evident also in the much larger metal–metal separation seen in our calculations on weakly coupled V-containing complexes than that found in an experimentally studied (monocationic) analogue. Our calculations on  $[(\text{dme})_3\text{VCl}_3\text{V}(\text{dme})_3]^+$ , a model for the latter species, return satisfactory agreement with experiment for the metal–metal and metal–ligand bonds but also indicate that the V–V distance is likely to be markedly susceptible to influences such as ligand modification (e.g. MeOH to dme to thf). In contrast, the species  $\text{M}_2(\text{dms})_3\text{Cl}_6^{2-}$  ( $\text{M} = \text{Nb}, \text{Ta}$ ), which are also models for crystallographically characterized structures, are found to possess robust triple bonds between metal atoms, in good agreement with experiment.

**Acknowledgment.** We gratefully acknowledge the Australian Research Council (ARC) for financial support.

**Note Added after ASAP:** The phrase “face-shared V(III) dimers” on the sixth page of the version of this paper posted ASAP on October 31, 2002, was incorrect. The correct phrase, “face-shared V(II) dimers”, is present in the version posted on November 13, 2002.

IC011250Z